CHAPTER VII
ELECTROPHORETIC DEPOSITION OF TITANIUMDIOXIDE/PURIFIED SODIUM-BENTONITE COMPOSITES FOR DSSC ELECTRODES

7.1 Abstract

The electrophoretic deposition (EPD) was employed to prepare TiO_2/clay composites for photoanodes in dye-sensitized solar cells. Mixture of synthesized TiO_2 and commercial P25 was utilized as TiO_2 source. The extracted red cabbaage dye was used as a sensitizer and clay was Na-bentonite. Various clay contents indeposited films were investigated while the ratio of synthesized TiO_2 and P25 was kept at 50:50 mole ratio as starting mixture. The starting clay contents in synthesized TiO_2 are 0, 5, 10 and 20 wt.%. The clay contents in deposited films are 0, 2.4, 5.5, and 8.9 wt.% whereas the ratios of anatase and rutile phase in 0, 2.4, 5.5, and 8.9 wt.% clay composite films are 89:11, 87:13, 89:11, and 83:17, respectively. The amount of dye loading in composite films at high clay contents is greater than those at low clay contents. FE-SEM images reveal that the aggromerates of synthesized TiO_2 increase as clay content increases. In spite of the fact that the photovoltaic properties of cells frabicated with composite films decrease with increasing clay contents, 2.4 wt.% clay in composite film does not affects the cell performance compared to those of the cells with 5.5 and 8.9 mol% Si.

Keywords: Titanium dioxide; Clay; Red cabbage dye; Electrophoretic deposition; Photovoltaic properties

7.2 Introduction

Dye-sensitized solar cell (DSSC) or Grätzel's cell has been developed widely since it is promising for clean and sustainable energy, i.e. environmentally friendly, low cost, and comparable energy conversion efficiency, in particular, indoor application. The Grätzel's cell is mainly composed of dye acting as light sensitizer or electron source, highly porous semiconductor for supporting dye which is usually TiO_2, p-type semiconductor or electrolyte, and catalyst (platinum, graphite, gold,

etc.) for regenerating electron or reduced species at back electrode. All these components are equally necessary to provide a high efficient cell.

The main problem of a low DSSC efficiency is electron recombination at the surface of semiconductor where a lot of trap states (Frank 2004; Ofir, 2006; Kopidakis 2006; Tennakone et al., 2003) locate. Several methods such as tailoring dye molecules (Zakeeruddin *et al.* 2009), adding co-adsorbates with dyes (Wang, 2003; Wang, 2004; Zhang, 2005), and adding additives in electrolyte (Nazeeruddin, 1993; Kopidakis, 2006), have succeeded in retarding recombination process. Besides, this could be achieved via ultrathin coated TiO_2 surface by higher conduction band edge of metal oxide (Kong et al., 2007), such as Nb_2O_5 (Chen *et al.*, 2001), ZnO (Wang *et al.*, 2001), SrO (Yang *et al.*, 2002), $SrTiO_3$ (Diamante *et al.*, 1977). The higher conduction band edge of these metal oxide acts as an insulator between injected electron and triiodide, leading to increase the electron density of conduction band of TiO_2 and then improve open-circuit voltage and overall cell performances. In addition, to reducing the recombination rate, Lee *et al.*, (2006) found that $CaCO_3$ coated TiO_2 increased the adsorption amount of dye molecules and then improved photocurrent density. In fact, the better dye adsorption is obtained with the basic oxide (Kay and Grätzel, 2002), such as MgO (IEP at pH 12) (Jung *et al.*, 2005), Al_2O_3 (IEP at pH 9) (Palomares *et al.*, 2003), Y_2O_3 (IEP at pH9) along with $CaCO_3$ (IEP at pH 8.2) (Lee *et al.*, 2006).

Interestingly, Nguyen *et al.* (2007) reported the TiO_2/SiO_2 nanocomposite fabricated by EPD improved photovoltaic properties of the cells. They believed that this was attributed to the electrostatic interaction between TiO_2 and SiO_2 particles which took place via electrophoretic process. Consequently, bentonite mineral, a kind of natural clay, is promising to be an energy barrier owing to its interesting structure possessed of aluminosilicate with high aspect ratio. In the previous studies (Saelim *et al.*, 2011a; Saelim *et al.*, 2011b; Chapter VI), only at low clay contents the TiO_2/clay composite films prepared by doctor blading technique did not diminish much the cell performances. This was attributed to the quite evident of its insulation property. As a result, it challenges us to observe the improvement of the photovoltaic properties of the DSSC owing to the contribution of the electronic contact between TiO_2 and Na-bentonite by using EPD technique.

In this study the purified Na-bentonite was used to fabricate the TiO_2/clay composites as electrode for dye-sensitized solar cells by cathodic electrophoretic deposition. Various bentonite contents were employed. The combination of synthesized TiO_2 and commercials P25 were utilized as TiO_2 source. Extracted red cabbage dye was used as the sensitizer of the DSSCs. The clay contents in deposited films were examined. Also, the important roles of clay in the deposited films would be discussed.

7.3 Experimental

7.3.1 Materials

Na-bentonite, 70% purity was kindly supplied from Thai Nippon Chemical Industry Co., Ltd, Thailand. Commercial P25 TiO_2 powder was from Degussa. Diisopropoxytitanate bis(acetylacetonate), 75 wt.% solution in isopropyl alcohol was from Aldrich. LiI, 99%, 4-tert-butylpiridine, 96% and chloroplatinic acid hydrate ~38% Pt-basis were from Sigma-Aldrich, and I_2 was from Suksapan panish, Thailand. Valeronitrile, 98% and Guanidine thiocyanate, 99% were from ACROS. Acetonitrile was from Loba chemie. Nitric acid, 65% and absolute ethanol were purchased from RCI-Labscan Ltd.

7.3.2 Preparation of Red Cabbage Dye Sensitizer

Fresh red cabbage leaves were cut into very small pieces and then extracted in a ethanol/water (9:1 by volume) mixed solvent. Afterward, the solid residues were filtered out. Then, the dye solution was concentrated by a rotary evaporator at 50 °C and finally stored at 4 °C prior to use.

7.3.3 Preparation of Purified Na-Bentonite

Raw Na-bentonite was purified more by swelling in deionized water with 60 times by weight under vigorous stirring for 12 h. The swollen Na-bentonite was settled for 2 weeks. The impurity settled compactly at the bottom while only the highly dispersed swollen Na-bentonite on the top, which had the main compositions of 78.5 wt.% SiO_2, 16.4 wt.% Al_2O_3, 2.4 wt.% Fe_2O_3, and 1.7 wt.% MgO obtained

from the X-ray fluorescence analysis, was collected, dried, and ground in mortar. The purified Na-bentonite was attained.

7.3.4 Preparation of Photoanodes

TiO_2 sols was prepared by hydrolyzing 2.5 g of diisopropoxytitanate bis(acetylacetonate) with 15 ml of water in case of 100% sol TiO_2 and 5 ml of water in case of TiO_2/clay composites. The solution was heated to 75°C and then 0.1 ml of 10-times diluted 65% HNO_3 was dropped into the solution before kept heating until it became transparent. The purified Na-bentonite (5, 10, and 20 wt.% clay of mixture with TiO_2 sol) was swollen in 10 ml of RO water overnight before mixing with the TiO_2 sols at 70°C for 1 h. In case of 20-ben, another 0.1 ml of nitric acid was added during the mixing to ensure the complete formation of TiO_2 sol and reduce the co-aggregation of purified clay and sol. To prepare the colloid suspension for electrophoresis, the sol-TiO_2/clay suspensions were mixed with P25 powder with 1:1 sol-Ti: P25-Ti molar ratio and then the mixtures were diluted in absolute ethanol to obtain 5 g/l of TiO_2. The mixtures were stirred vigorously over night and subsequently kept under sonication for 10 min. The cathodic EPD was conducted around 0 °C (Tirosh et al., 2006). The fluorine-doped SnO_2 (FTO) glasses were employed on both electrodes. The voltage of 12V controlled by DC-source, regulated: 0-30V (Kenji, model K-01) was used throughout the experiment with the constant distance between electrodes at 0.5 cm. Likewise, The deposition time was 2.5 min and dried at 400 °C for 15 min for each layer. The deposited films were sinter at 500 °C in air for 1 h. Then, they were immersed into the extracted red cabbage dye solution for 20 h to obtain the photoanode films.

7.3.5 Cell Assembly

The Pt cathode film was prepared by spreading 1 drop of 10 mM chloroplatinic acid hydrate in 2-propanol by the doctor blading method on fluorine-doped SnO_2 (FTO) glasses, TEC 15 and annealed at 400 °C for 15 min. The electrolyte consisting of 0.3 M LiI, 0.03 M I_2, 0.5 M 4-tert-butylpiridine, and 0.1 M Guanidine thiocyanate in acetonitrile and valeronitrile (85:15 volume ratio) was

dropped and spread thoroughly between the two electrodes. Two clips were used to camp two electrodes together. The photoanodes were masked by using black mask with the open active area of 0.3 cm^2. The photovoltaic measurement was performed suddenly after electrolyte spreading.

7.3.6 Characterization and Measurement

The morphology of deposited films and the metal element composition were characterized by using a field emission scanning electron microscope (FE-SEM, Hitachi S4800) equipped by energy dispersive X-ray analyzer (EDX). The phase fraction of anatase and rutile was determined by X-ray diffractometer (XRD, Bruker Model-D8 Advance) with the Topas program. The scan was from 2-Theta of 20 to 60. The UV-visible spectrophotometer (UV-2550, Shimadzu) was employed to observe amount of adsorbed dye on the deposited film. For the film thickness measurement, the step profile, Vecco Dektak 150 was used. The photovoltaic properties of the prepared DSSCs, i.e. short circuit current (J_{sc}, mA/cm^2), open circuit voltage (V_{oc}, V), fill factor (FF), and efficiency (ŋ, %), were determined from the I–V curve obtained by using a digital Keithley 236 multimeter under an irradiation of white light from a 1000 W/HS Xenon arc lamp (Super solar simulator, Wacom: WXS-155S-L2, AM 1.5 GMM) with a 100 mW/cm^2 light intensity, where the fill factor and efficiency were calculated based on the following equations:

$$FF = \frac{J_{max} \times V_{max}}{J_{sc} \times V_{oc}} \tag{7.1}$$

$$\eta = \frac{J_{sc} \times V_{oc} \times FF}{P_{in}} \tag{7.2}$$

where J_{max} is maximum power point current (mA/cm^2), V_{max} is maximum power point voltage (V), and P_{in} is power of incident light (mW/cm^2).

7.4 Results and Discussion

The composite films with 0, 5, 10, 20 wt.% of purified Na-bentonite mixed with synthesized TiO_2 are defined as 0-ben, 5-ben, 10-ben, and 20-ben. Since Na-bentonite swells in water only and does not swell in lower polar solvent such ethanol used for electrophoretic media (Grinis *et al.*, 2008) in this study, the first mixed with synthesized TiO_2 could be the best way to enhance the dispersion of clay particles. In fact, the TiO_2 sols are readily for EPD without any charging reagent (Grinis *et al.*, 2008; Zhitomirsky, 2002) since it has already been stabilized with positive charges of protons form nitric acid and water, and with acetyl acetone. However, the particle size of sols are around 5-10 nm, leading to ease of crack formation on the deposited film. Therefore, the addition of P25 with the particle size around 25 nm (Nazeeruddin *et al.*, 1993) would decrease the macro-crack formation which makes poor adherence between films and FTO glasses, and then lower the cell performances. Therefore, P25 could act as binder of synthesized TiO_2 colloids, which is described in Ngamsinlapasathian *et al.* (2006) study. Besides the proton and acetyl aceton in TiO_2, sol solution can behave as charging reagents for P25 to facilitate deposition of P25 on the cathode.

7.4.1 Crystal Phase Composition of TiO_2

The phase fraction of anatase and rutile in the composites films, 0-ben, 5-ben, 10-ben, and 20-ben calculated from the total area under the X-ray diffraction patterns are 89:11, 87:13, 89:11, and 83:17, respectively. It seem that the anatase and rutile fractions in the composites are not different significantly apart from that of 20-ben. The higher amount of rutile phase in 20-ben is resulted from the double nitric acid addition in the mixture of TiO_2 sol and swollen clay to reduce the large aggregates since higher acid concentration can influence to the phase formation of TiO_2 sol (Dai *et al.*, 2010, Wang and Ying, 1999).

7.4.2 Deposited Film Composition

The compositions of clay in composite films were calculated from the Si mole percents from EDX data. The clay and Si contents in deposited films compared with various clay contents in starting mixture are shown in Table 7.1. The clay contents in deposited film of 5-ben is slightly lower than that in starting mixture while that of 20-ben is quite lower and 10-ben is slightly higher. This trend agrees with anatase fractions since Na-bentonite was loaded into synthesized TiO_2 before mixed with P25. It means that clay particles are coated with synthesized TiO_2 as shown in Fig. 7.1a. However, if the clay contents in deposited film depended on the anatase fraction, the contents would be higher than those shown in Table 7.1, according to the anatase and rutile fraction of TiO_2. This is ascribed to the large aggregates of clay particles with synthesized TiO_2 precipitating instead of suspending in the media.

7.4.3 Deposited Film Morphology

In addition, the Fig. 7.2 shows the surface morphology of composite films, which exhibit the two different textures of TiO_2 from the different TiO_2 sources. The larger particles are possessed of P25 which has the particle size around 25 nm, and the fine particles are possessed of synthesized TiO_2 with particle size of around 5-10 nm as observed in the our previous work (Saelim *et al.*, 2011b). Besides, more aggregation of synthesized TiO_2 was found with more clay contents.

Furthermore, the pin holes with the sizes around 0.5-1 μm are found in the deposited films as depicted in the Fig. 7.2e. These holes took place from the gas bubbles forming in the electrolysis reaction of water when high voltage is employed. The reactions are shown in eq. 7.3 and 7.4.

$$\text{Anode: } 2H_2O \rightarrow O_2(gas) + 4H(+) + 4e(-) \quad (7.3)$$

$$\text{Cathode: } 4H_2O + 4e(-) \rightarrow 4OH(-) + 2H_2(gas) \quad (7.4)$$

Tabellion *et al.*, (2004) reported that a large amount of water in the suspension and high voltage applied can provide large pin holes with poor film adherence and lack of film uniformity. With water content of about 10 % by volume,

the films contain small holes and have good film adherence and uniformity on the substrate. Besides water, protons from nitric acid added to catalyze sol formation can be reduced and generate hydrogen gas at cathode. However, some of protons in the mixture at high clay content were neutralized with hydroxide ion generated by purified clay. Therefore, larger number of excess protons in 0-ben generated larger holes and larger number of holes in the films than those composites.

EPD could be a binder-free technique used for DSSC applications which needs to avoid high temperature treatment (Miyasaka *et al.*, 2002; Miyasaka *et al.*, 2004). Nevertheless, without any binders, the crack formation takes place when too thick deposited film is formed within the single step. The multiple depositions can solve this problem (Chiu *et al.*, 2011; Grinis *et al.*, 2008). In this study, it is observed that the macro-cracks forming at earlier layers can turn in to micro-crack or disappear at the next layers when the deposited film is thicker. The FE-SEM images are shown in Fig. 7.3. This result agrees with the study of Chiu *et al.* (2011).

7.4.4 Dye Loading

To compare the dye loading in deposit films, UV-vis spectra of dye molecule adsorbed on deposited films were investigated as shown in Fig. 7.4. All the spectra of dye adsorbed on composite film show evidently red shift as compared to that of dye in solution. The 10-ben composite gives the highest dye loading corresponding to the highest absorbance at the wavelength of maximum absorbance. According to the FE-SEM images in Fig. 7.2 and the phase fraction, the higher dye loading of 10-ben and 20-ben composites was ascribed to the increase in clay contents which influence the specific surface area of composite as described in the our previous work (Saelim *et al.*, 2011a; Saelim *et al.*, 2011b; Chapter VI). However, dye loading of 20-ben is slightly lower than that of 10-ben, which is the same as the comparison between 0-ben and 5-ben. This is due to the lower anatase fraction in 20-ben composite as well as the slightly lower of that in 5-ben. As the anatase crystal has higher surface area than rutile crystal due to the smaller crystal of anatase.

7.4.5 Photovoltaic Properties

The photovoltaic properties of DSSC with 0-ben, 5-ben, 10 ben, and 20 ben were shown in Fig. 7.5. Even though the conversion efficiency decreases with increasing clay content, the 5-ben retains the high DSSC performance as 0-ben. The maximum DSSC performance, J_{sc}, V_{oc}, ff, and ŋ, of 5-ben is 2.1 mA/cm^2, 0.55 V, 0.72, and 0.83%, respectively. The natural clay, Na-bentonite enhances the recombination rate as the voltage decreases (Tennakone *et al.*, 2003) with increasing clay content since their insulation property resists the charge transport in the deposited films. This leads to lower overall performances of the DSSCs. The dense of aggregate clay aligns in perpendicular of charge transfer in composite film at high clay content as depicted in Fig. 7.1b.

The optimal film thickness is found around 7-9 μm which is less than those of DSSC sensitized with ruthenium based dyes (Haung *et al.*, 2006; Ito *et al.*, 2008; Ito *et al.*, 2009; Wang *et al.*, 2004a). This is explained by the short length of electron diffusion (Haung *et al.*, 2006) or short of electron life time (Jang *et al.*, 2009) in deposited films due to the fast recombination rate (Kay, 1994) which usually occurs with natural dyes.

Indeed, the only ultrathin coating of insulators about 1-5 nm could retard the recombination (Chen *et al.*, 2001; Lee *at al.*, 2006). The thickness of stack clay platelets as shown in Fig. 7.1a is still beyond the optimum thickness for energy barrier to retard the charge recombination. The high energy equipment is probably needed to disrupt the aggregate or stack of clay platelets (Inoue *et al.*, 2010). Furthermore, this would help to reduce the size of clay platelets that obstruct the charge and ion transport in the photoanode film. The use of small size of clay platelet such as synthetic clay is also interesting (Inoue *et al.*, 2010; Park *et al.*, 2008).

7.5 Conclusions

TiO_2/purified Na-bentonite composite films for photoanodes in dye-sensitized solar cells were prepared by the electrophoretic deposition. The anatase TiO_2 and purified Na-bentonite from the mixture of synthesized TiO_2/ purified Na-bentonite suspension enhance dye adsorption in the deposited films. In this study Na-

bentonite did not show any roles of energy barrier to reduce charge recombination. However, the techniques used to break more clay aggregation and clay stack in order to obtain high dispersion of clay pletelet with the suitable thickness for energy barrier function are still very challenging since at low clay content, 3.1 mole% Si or 2.4 wt.% clay in deposited film achieves the high cell performance as electrode without clay.

7.6 Acknowledgments

This work was financially supported by the Royal Golden Jubilee Ph.D. Program, Thailand; Rachadapiseksompote Endowment, Chulalongkorn University, Thailand; and National Nanotechnology Center, National Science and Technology Development Agency, Thailand. The authors would like to thank Thai Nippon Chemical Industry Co., Ltd for kindly providing the clay and thank Prof. Michael Grätzel and Laboratory for Photonics and Interfaces for the kindly supplying FTO glasses

7.7 References

Chen, S.G., Chappel, S., Diamant, Y., and Zaban, A. (2001). Preparation of Nb_2O_5 coated TiO_2 nanoporous electrodes and their application in dye-sensitized solar cells. Chemistry of Materials, 13(12), 4629-4634.

Chiu, W.-H.., Lee, K.-M., Hsieh, and W.-F. (2011). High efficiency flexible dye-sensitized solar cells by multiple electrophoretic depositions. Journal of Power Sources, 196(7), 3683-3687.

Dai, S., Wu, Y., Sakai, T., Du, Z., Sakai, H., and A., Masahiko. (2010). Preparation of highly crystalline TiO_2 nanostructures by acid-assisted hydrothermal treatment of hexagonal-structured nanocrystalline titania/cetyltrimethyammonium bromide Nnanoskeleton. Nanoscale Research Letters, 5(11), 1829-1835.

Diamante, Y., Chen, S.G., Melamed, O., and Zaban, A. (2003). Core–shell nanoporous electrode for dye-sensitized solar cells: the effect of the $SrTiO_3$ shell on the electronic properties of the TiO_2. The Journal of Physical Chemistry B, 107(9), 1977-1981.

Frank, A. J., Kopidakis, N., and van de Lagemaat, J. (2004). Electron in nanostructured TiO_2 solar cells: transport, recombination and photovoltaic properties. Coordination Chemistry Reviews, 248(13-14), 1165-1179.

Ginis, L., Dor, S., Ofir, A., and Zaban, A. (2008). Electrophoretic deposition and compression of titania nanoparticle films for dye-sensitized solar cells. Journal of Photochemistry and Photobiology A: Chemistry, 198(1), 52–59.

Huang, C.-Y., Hsu, Y.-C., Chen, J.-G., Suryanarayanan, V., Lee, K.-M., Ho., K.-C. The effects of hydrothermal temperature and thickness of TiO_2 film on the performance of a dye-sensitized solar cell. Solar Energy Materials & Solar Cells, 90 (15), 2391–2397.

Inoue, T., Uchida, S., Kubo, T., and Segawa, H. (2010). High performance quasi-solid dye-sensitized solar cells with nano-clay electrolyte. Materials Research Society Symposium Proceedings, 1211, 87-90.

Ito, S., Murakami, T.N., Comte, P., Liska, P., Grätzel, C., Nazeeruddin, M.K., and Grätzel, M. (2008). Fabrication of thin film dye-sensitized solar cells with solar to electric power conversion efficiency over 10%. Thin Solid Films, 516(14), 4613-4619.

Ito, S., Nazeeruddin, M.K., Zakeeruddin, S.M., Péchy, P., Comte, P., Grätzel, M., Mizuno, T., Tanaka, A., and Koyanagi, T. (2009). Study of dye-sensitized solar cells by scanning electron micrograph observation and thickness optimization of porous TiO_2 electrodes. International Journal of Photoenergy, No. 517609.

Jang, S.-R., Yum, J.-H., Klein, C., Kim, K.-J., Wagner, P., Officer, D., Grätzel, M., and Nazeeruddin, M. K. (2009). High molar extinction coefficient ruthenium sensitizers for thin film dye-sensitized solar cells. The Journal of Physical Chemistry C, 113(5), 1998–2003.

Jung, H. S., Lee, J.-K., Nastasi, M., Lee, S.-W., Kim, J.-Y., Park, J.-S., and Hong, K. S. (2005). Preparation of nanoporous MgO-coated TiO_2 nanoparticles and their application to the electrode of dye-sensitized solar cells. Langmuir, 21(23), 10332–10335.

Kay, A. (1994). Solar cell based on nanocrystalline TiO_2 electrodes. Ph.D. Dissertation, Ecol Polytechnique fédérale de Lausanne (EPFL), Lausanne.

Kay, A., and Grätzel, M. (2002). Dye-sensitized core-shell nanocrystals: improved efficiency of mesoporous tin oxide electrodes coted with a thin layer of an insulating oxide. Chemistry of Materials, 14(7), 2930-2935.

Kong, F.-T., Dai, S.-Y., and Wang, K.-J. (2007). Review of recent progress in dye-sensitized solar cells. Advances in OptoElectronics, No. 75384.

Kopidakis, N., Neale, N. R., and Frank, A. J. (2006). Effect of an adsorbent on recombination and band-edge movement in dye-sensitized TiO_2 solar cells: evidence for surface passivation. Journal of Physical Chemistry B, 110(25), 12485-12489.

Lee, S., Kim, J. Y., Honga, K. S., Jung, H. S., Lee, J.-K., and Shin, H. (2006). Enhancement of the photoelectric performance of dye-sensitized solar cells by using a $CaCO_3$-coated TiO_2 nanoparticle film as an electrode. Solar Energy Materials & Solar Cells, 90(15), 2405–2412.

Ofir, A., Dittrich, Th., Tirosh, S., Grinis, L., and Zaban, A. (2006). Influence of sintering temperature, pressing, and conformal coatings on electron diffusion in electrophoretically deposited porous TiO_2, Journal of Applied Physics, 100(7), 074317.

Miyasaka, T., Kijitori, Y., Murakami, T. N., Kimura, M., and Uegusa, S. (2002). Efficient nonsintering type dye-sensitized photocells based on electrophoretically deposited TiO2 layers. Chemistry Letters, 31(12), 1250–1251.

Miyasaka, T., and Kijitori, Y. (2004). Low-temperature fabrication of dye-sensitized plastic electrodes by electrophoretic preparation of mesoporous TiO2 layers. Journal of the Electrochemical Society, 151(11), A1767–A1773.

Nazeeruddin, M.K., Kay, A., Rodicio, I., Humphry-Baker, R., Müller, E., Liska, P., Vlachopoulos, N., and Grätzel, M. (1993). Conversion of light to electricity

by *cis*-X_2bis(2,2'-bipyridyl-4,4'-dicarboxylate)ruthenium(II) charge-transfer sensitizers (X = Cl^-, Br^-, I^-, CN^-, and SCN^-) on nanocrystalline TiO_2 electrodes. Journal of the American Chemical Society, 115(14), 6382-6390.

Ngamsinlapasathian, S., Pavasupree, S., Suzuki, Y., and Yoshikawa, S. (2006). Dye-sensitized solar cell made of mesoporous titania by surfactant-assisted templating method. Solar Energy Materials & Solar Cells, 90(18-19), 3187-3192.

Nguyen, T.-V., Lee, H.-C., Alam Khan, M., and Yang, O.-B. (2007). Electrodrposition TiO_2/SiO_2 nanocomposite for dye-sensitized solar cell. Solar Energy, 81(4), 529-534.Palomares, E., Clifford, J. N., Haque, S. A., Lutz, T., and Durrant, J. R. (2003). Control of charge recombination dynamics in dye-sensitized solar cells by the use of conformally deposited metal oxide blocking layers. Journal of the American Chemical Society, 125(2), 475–482.

Park, J. H., Kim, B.-W., and Moon, J. H. (2008). Dual functions of clay nanoparticles with high aspect ratio in dye-sensitized solar cells. Electrochemical and Solid-State Letters, 11(10), B171-B173.

Saelim, N.-o., Magaraphan, R., and Sreethawong, T. (2011). TiO_2/modified natural clay semiconductor as a potential electrode for natural dye-sensitized solar cell, Ceramics International, 37(2), 659-663.

Saelim, N.-o., Magaraphan, R., and Sreethawong, T. (2011). Preparation of sol–gel TiO_2/purified Na-bentonite composites and their photovoltaic application for natural dye-sensitized solar cells. Energy conversion Management, 52(8-9), 2815–2818.

Tabellion, J., and Clasen, R. (2004). Electrophoretic deposition from aqueous suspensions for near-shape manufacturing of advanced ceramics and glasses-applications. Journal of Materials Science, 39(3), 803-811.

Tennakone, K., Jayaweera, P.V.V., and Bandaranayake, P.K.M. (2003). Dye-sensitized photoelectrochemical and solid-state solar cells: charge separation, transport and recombination mechanisms. Journal of Photochemistry and Photobiology A: Chemistry, 158(2-3), 125–130.

Tirosh, S., Dittrich, T., Ofir, A., Grinis, L., and Zaban, A. (2006). Influence of ordering in porous TiO_2 layers on electron diffusion. The Journal of Physical Chemistry B: Letters, 110(33), 16165-16168.

Wang, C. -C., and Ying, J. Y. (1999). Sol-gel synthesis and hydrothermal processing of anatase and rutile titania nanocrystals. Chemistry of Materials, 11(11), 3113-3120.

Wang, Z. -S., Huang,C. -H., Hang, Y. -Y., Hou, Y. -J., Xie, P. -H., Zhang, B. -W., and Cheng, H. -M. (2001). A Highly Efficient Solar Cell Made from a Dye-Modified ZnO-Covered TiO_2Nanoporous Electrode. Chemistry of Materials, 13(2), 678-682.

Wang, P., Zakeeruddin, S. M., Comte, P., Charvet, R., Humphry-Baker, R., and Grätzel, M. (2003d). Enhance the performance of dye-sensitized solar cells by co-grafting amphiphilic sensitizer and hexadecylmalonic acid on TiO_2 nanocrystals. The Journal of Physical Chemistry B, 107(51), 14336-14341.

Wang, P., Zakeeruddin, S. M., Humphry-Baker, R., and Grätzel, M. (2004b). A binary ionic liquid electrolyte to achieve > 7% power conversion efficiencies in dye-sensitized solar cells. Chemistry of Materials, 16(14), 2694-2696.

Wang, Z.-S., Kawauchi, H., Kashima, T., and Arakawa, H. (2004). Significant influence of TiO_2 photoelectrode morephology on the energy conversion efficiency of N719 dye-sensitized solar cell. Coordination Chemistry Reviews, 248(13-14), 1381-1389.

Yang, S., Huang, Y., Huang, C., and Zhao, X. (2002). Enhanced Energy Conversion Efficiency of the Sr^{2+}-Modified Nanoporous TiO_2 Electrode Sensitized with a Ruthenium Complex. Chemistry of Materials, 14(4), 1500-1504.

Zakeeruddin, S.M., and Grätzel, M. (2009). Solvent-free ionic liquid electrolytes for mesoscopic dye-sensitized solar cell. Advanced Functional Materials, 19(14), 2187-2202.

Zhang, Z., Zakeeruddin, S. M., O'Regan, B. C., Humphry-Baker, R., and Grätzel, M. (2005). Influence of 4-Guanidinobutyric Acid as Coadsorbent in Reducing

Recombination in Dye-Sensitized Solar Cells. Journal of Physical Chemistry B, 109(46), 21818-21824.

Zhitomirsky, I. (2002). Cathodic electrodeposition of ceramic and organoceramic materials. Fundamental aspects. Advances in Colloid and Interface Science, 97(1-3), 279-317.

Table 7.1 The Si and clay contents in deposited films from EDX data compared with clay contents in starting mixture

Batch	wt.% clay as starting	% mole Si after deposited	wt.% clay after deposited
0-ben	0	0	0
5-ben	2.6	3.1	2.4
10-ben	5.3	7.2	5.5
20-ben	11.1	11.3	8.9

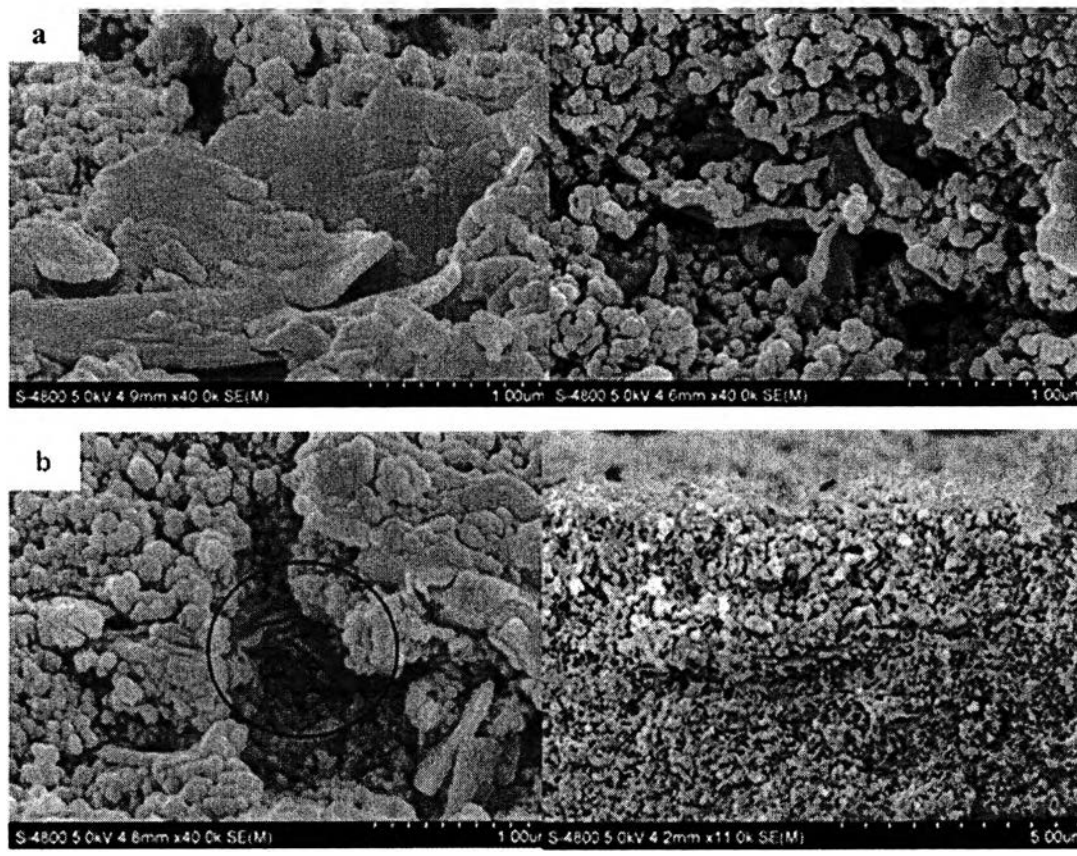

Figure 7.1 The crossectional-viewed FE-SEM micrographs of composite film.

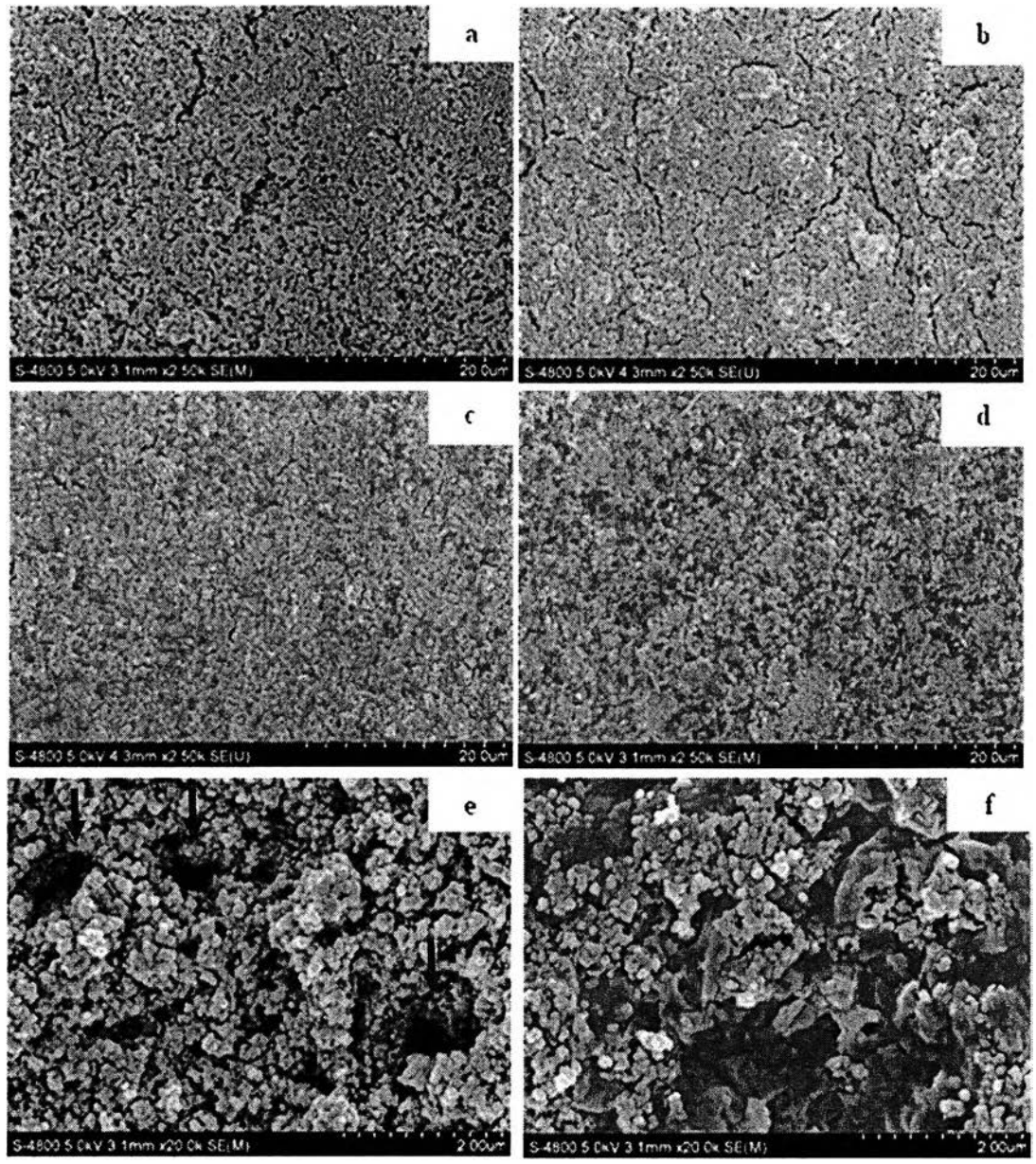

Figure 7.2 Top-viewed FE-SEM micrographs of (a) 0-ben, (b) 5-ben, (c) 10-ben, (d) 20-ben, and magnified micrograph of (e) 0-ben with arrow heads indicating large pinholes and (f) 20-ben.

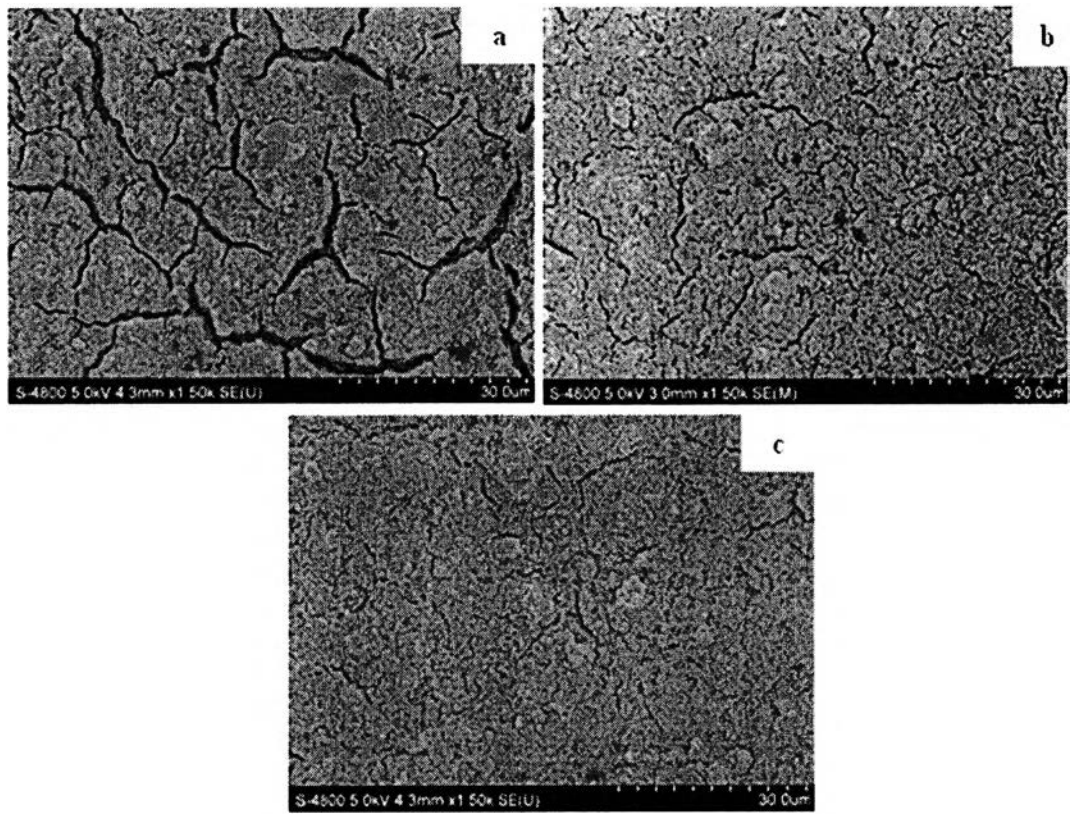

Figure 7.3 Top-viewed FE-SEM micrographs of (a) 4 μm at 4th layer, (b) 5.5 μm at 5th layer, and (c) 12.5 μm at 12th layer.

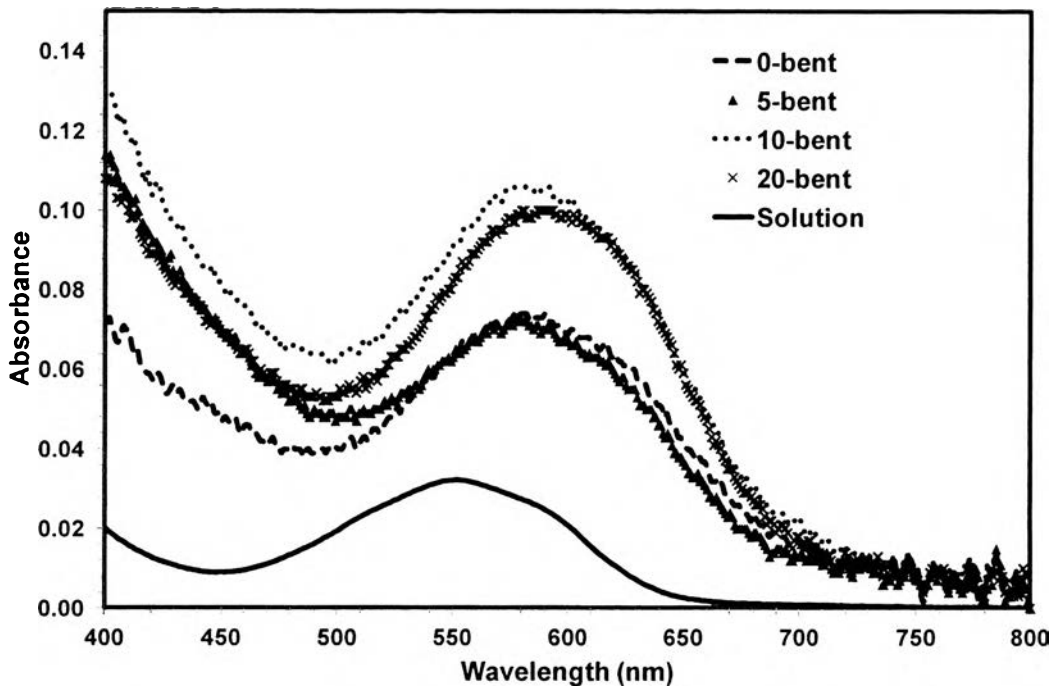

Figure 7.4 The spectra of red cabbage dye adsorbed on deposited films with the subtraction of deposited films and glass substrates.

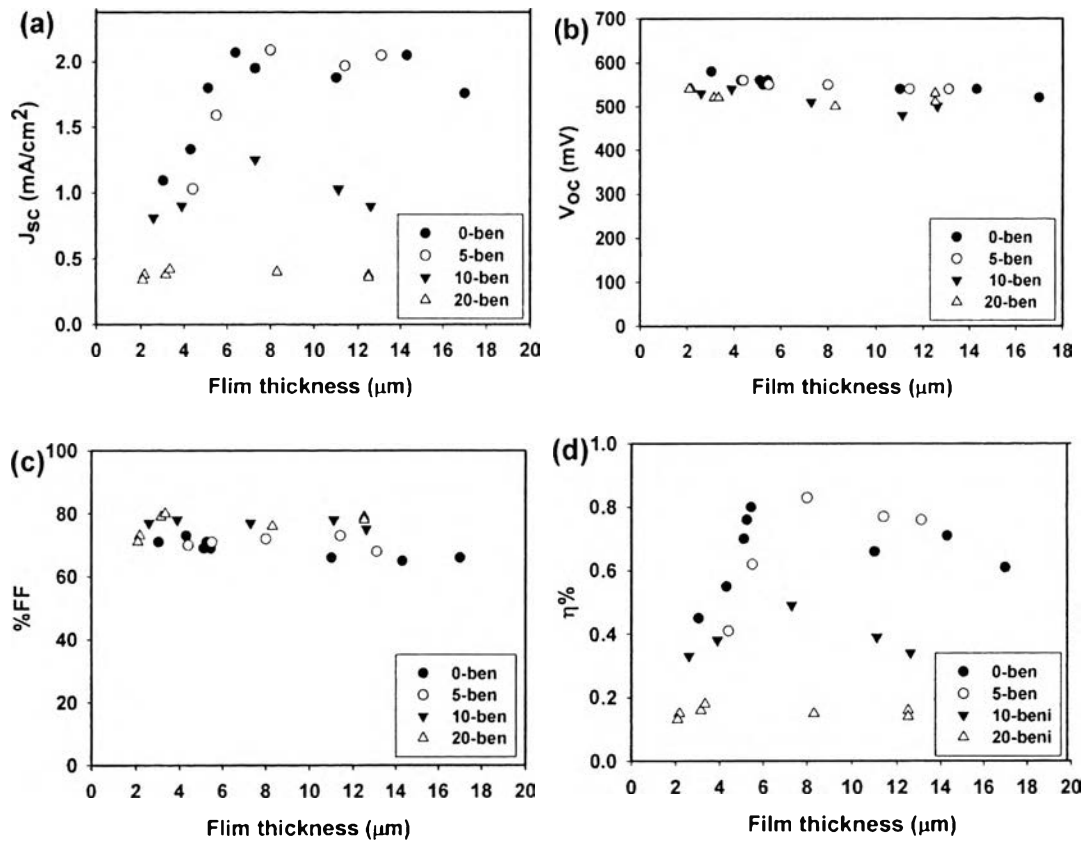

Figure 7.5 The photovoltaic properties, (a) short circuit current, J_{sc}, (b) open circuit voltage, V_{oc}, (c) fill factor, FF, and (d) conversion efficiency, ŋ% of DSSC with TiO_2/clay composite electrodes at various clay contents and film thicknesses.